EXPERIMENTAL DETERMINATION OF ADDED HYDRODYNAMIC RESISTANCE CAUSED BY MARINE BIOFOULING ON SHIPS

Yigit Kemal Demirel, Department of Naval Architecture, Ocean and Marine Engineering, University of Strathclyde, Glasgow, United Kingdom
Osman Turan, Department of Naval Architecture, Ocean and Marine Engineering, University of Strathclyde, Glasgow, United Kingdom
Sandy Day, Department of Naval Architecture, Ocean and Marine Engineering, University of Strathclyde, Glasgow, United Kingdom

This paper presents a novel experimental approach towards establishing a method to predict the added resistance caused by the calcareous fouling. An extensive series of towing tests using the flat plates covered with artificial, 3D printed barnacles were carried out at the Kelvin Hydrodynamics Laboratory (KHL) at the University of Strathclyde. The tests were designed to examine the effects of 2 different fouling parameters, namely the coverage percentage and locations of the fouling accumulation, over a range of Reynolds numbers.

The paper presents the added resistance due to calcareous fouling in terms of added frictional coefficient for a surface coverage of fouling for up to 20%, and for a surface coverage of different spatial heterogeneous fouling for a constant 5% over different speeds (Reynold numbers).

1. Introduction

In the quest to achieve the targeted carbon emissions as well as improving the energy efficiency of ships, the maritime industry has been studying, experimenting and applying various technological and operational measures, including alternative fuels, energy saving devices, as well as antifouling coatings. It was indicated in the IMO's Green House studies [1] that up to 85% of the practically available energy on board is utilised to overcome the hydrodynamic forces, and 50% of the energy is consumed by hull resistance. Moreover, 80% of the overall resistance is caused by the frictional resistance of the hull. Hull roughness, due to the coating and the biofouling, plays a significant role on the resistance. Schultz [2] reported that heavy calcareous (like barnacles) fouling can lead up to an 86% increase in the shaft power requirements for the same speed.

Recognising this problem, coating companies have been trying to develop various types of antifouling coating to prevent/minimise the biofouling. However, the study as part of EU FP7 project Foul-X-Spel (Environmentally Friendly Anti-fouling Technology to Optimise the Energy Efficiency of Ships, Project no.285552, FP7-SST-2011-RTD-1), clearly demonstrated that the level of biofouling varies depending on the temperature and hence location, ship speed, time, as well as the type of antifouling. This finding is supported by many drydock reports, as well as hull fouling monitoring reports, which show that fouling levels vary significantly and this which makes it difficult to formulate the added resistance due to fouling.

With the aim of developing a scientific and fundamentally sound approach for predicting the effect of biofouling on added resistance, and hence the increase in power requirements, this

paper presents a novel experimental approach towards establishing a method to predict the added resistance caused by the calcareous fouling.

Different sizes of actual barnacles, which represent time based fouling, were scanned in 3D in order to model the barnacles in a digital environment. The digital models of barnacles were then printed in 3D by using 3D printing technology. The artificial barnacles were glued onto the surface of the flat plates. This technique provides a unique opportunity to determine the different fouling rates and locations on the hydrodynamic resistance of plates systematically. This systematic approach also eliminates the problems and uncertainties, which are encountered during the transportation of the immersed plates from the sea to the tank, including the transfer of the marine life from seawater to freshwater.

An extensive series of towing tests using the flat plates covered with artificial, 3D printed barnacles were carried out at the Kelvin Hydrodynamics Laboratory (KHL) at the University of Strathclyde. The tests were designed to examine the effects of 2 different fouling parameters, namely the coverage percentage and locations of the fouling accumulation, over a range of Reynolds numbers.
3 different coverage percentages of evenly distributions and 1 bare plate which serves as a reference plate are considered in the first sets of experiments as given below:

- Reference Plate 1 (Bare Plate)
- 5%
- 10%
- 20%

4 different locational accumulations and 1 bare plate which serves as a reference plate are considered while keeping the barnacle numbers constant such that the coverage area corresponds to 5%. The configurations of the second sets of the experiments are given below:

- Reference Plate 2
- Leading Edge
- Trailing Edge
- Middle
- Leading and trailing Edges

In total over 130 runs were carried out, including a series of repeat tests designed to quantify the uncertainty in the results. The drag coefficients of each surface were given in a comparative manner along with the uncertainty limits of the experiments.

Details of the experiments conducted in this study, namely experimental facilities, model details, test methodology and repeatability and uncertainty estimates are outlined below. The results of the experiments then are given separately for each set of tests and discussed in detail.

2. Experimental Facilities

As mentioned earlier, the experiments were carried out at the Kelvin Hydrodynamics Laboratory (KHL) of the University of Strathclyde. The KHL test tank has dimensions of 76.0 m x 4.6 m x 2.5 m. The tank is equipped with a digitally-controlled towing carriage,

state-of-the-art absorbing wavemaker, and a highly effective sloping beach. Fig. 1 shows a photo of the facility.

The carriage has a velocity range of 0 – 5 m/s, with the velocity range used in these experiments kept between 1.5 and 3.6 m/s. Fresh water was used in the experiments. The temperature of the water was monitored during the experiments in order to be able to evaluate drag coefficients according to the temperature.

Fig. 1 – The KHL towing carriage.

The overall drag values of each plate were measured using displacement transducers using the Linear Variable Differential Transformer (LVDT) principle. These transducers were acquired to ensure sensitive measurements of the resistance values, as well as to minimise the cross coupling of drag and side forces, since the differences of the resistance values between different surfaces were expected to be very small. It is of note that two transducers were used in the experiments; one for measuring the overall drag of the plates and one for checking the side forces. The intention was to keep the side forces effectively zero, to ensure the alignment of the plates.

Before the transducers were set on the plates, they were calibrated by hanging weights of known magnitude from the gauges and recording the output voltages for each weight. These two transducers were calibrated separately across the expected load range. It should be noted that the expected loads were predicted using CFD simulations similar to those performed in [3, 4]. The calibration factors were evaluated by obtaining the relationship between the load and output voltage.

3. Model Details and Preparations

The flat plates used for the tests were manufactured from 304 stainless steel grade sheet stock. Fig. 2 depicts the dimensions of the flat plates. The leading edges of the plates were shaped to a radius of 2.5 mm while the trailing edge was kept sharp in order to mitigate the extra drag due to the separation as much as possible. The flatness of the plates, as well as their dimensions, were checked using a CNC machine.

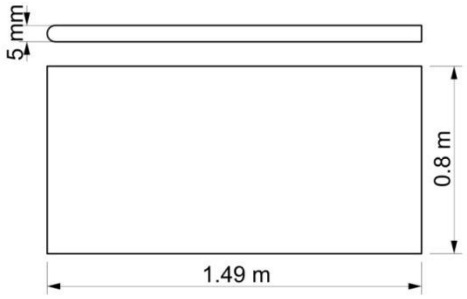

Fig. 2 – Dimensions of the flat plates.

The artificial barnacles used in the experiments were 3D printed using 3D scans of real barnacles. The real barnacles were bought and scanned using a 3D scanner system.

Individual barnacle models were created using the 3D scans of these barnacles. The most appropriate one, which corresponds to the real barnacles seen on ship hulls, was selected among them. An example of barnacles on a ship hull is seen in Fig. 3 [5].

Fig. 3 – Barnacles on a ship hull [5].

The selected model was then scaled based on the typical dimensions of the barnacles seen on ship hulls. Different sizes of barnacles were manufactured based on the observations on ship hulls and as well as based on the studies of Larsson, et al. [6] and Schultz [7]. A very large juvenile, which is 5 mm high, was chosen to be the working barnacle sample. A sample of barnacle models created for 3D printing system is shown in Fig. 4.

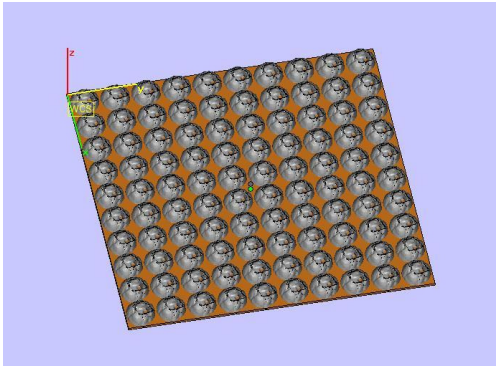

Fig. 4 – The artificial barnacle models.

Totally 2 plates were manufactured for the experiments. The surface conditions of the plates used in the experiments are explained below:

Reference Plate 1 was the plate which the artificial barnacles were glued onto for the first sets of experiments including 5%, 10% and 20% coverage percentages. Therefore, firstly reference plate 1 was towed in the tank when it was bare in order to obtain the baseline for the other configurations. Fig. 5 shows the reference plate 1 with marks on it. Following the completion of the tests for bare plate using the first reference plate, same plate was removed out of water and barnacles were glued to achieve 5% coverage and then put into water for the tests. Same procedure was repeated for 10% and 20 % surface coverage.

Fig. 5 – Reference Plate 1.

It is of note that the evenly distributions on the reference plate 1 was applied according to ASTM-D6990-05 [8].

Both sides plate 1 was covered with barnacles such that they cover 5% of the each wetted surface area. Fig. 6 shows Plate 1.

Fig. 6 – Plate 1.

Plate 2 was covered with barnacles such that they cover 10% of the each wetted surface area. Fig. 7 shows Plate 2.

Fig. 7 – Plate 2.

Plate 3 was covered with barnacles such that they cover 20% of the each wetted surface area. Fig. 8 shows Plate 3.

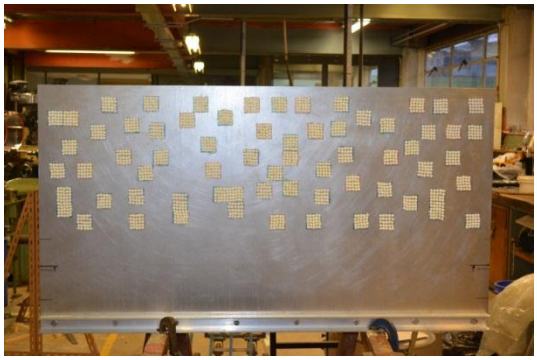

Fig. 8 – Plate 3.

Reference Plate 2 was the plate which the artificial barnacles were stuck on for the second sets of experiments including the fouling accumulations on leading edge, trailing edge, middle, leading and trailing edges while keeping the surface coverage to 5%. Therefore, firstly reference plate 2 was towed in the tank when it was bare in order to obtain the baseline for the other configurations. Fig. 9 shows the reference plate 2 with marks on it.

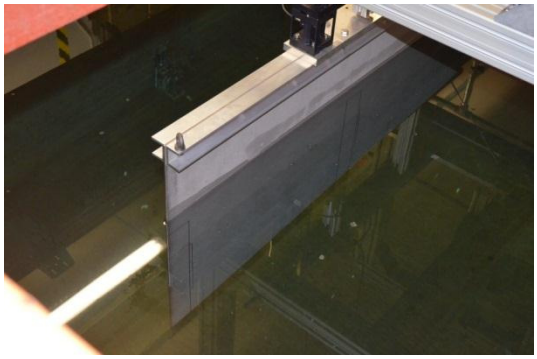

Fig. 9 – Reference Plate 2.

Plate 4 was the plate whose leading edge was covered with barnacles such that they cover 5% of the wetted surface area. Fig. 10 shows Plate 4.

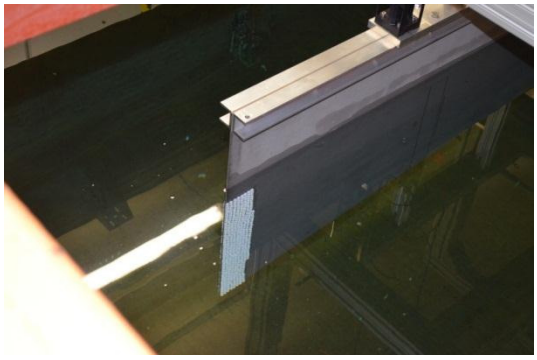

Fig. 10 – Plate 4.

Plate 5 was the plate whose trailing edge was covered with barnacles such that they cover 5% of the wetted surface area. Fig. 11 shows Plate 5.

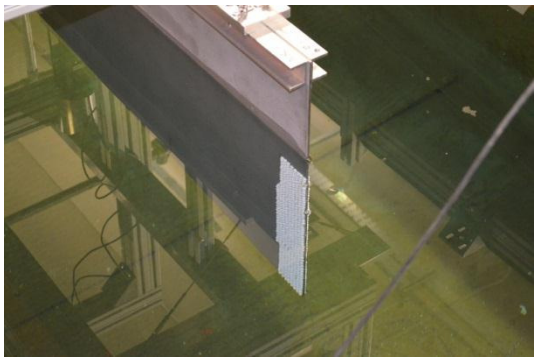

Fig. 11 – Plate 5.

Plate 6 was the plate whose middle was covered with barnacles such that they cover 5% of the wetted surface area. Fig. 12 shows Plate 6.

Fig. 12 – Plate 6.

Plate 7 was the plate whose leading and trailing edges were covered with barnacles such that they cover 5% of the wetted surface area. Fig. 13 shows Plate 7.

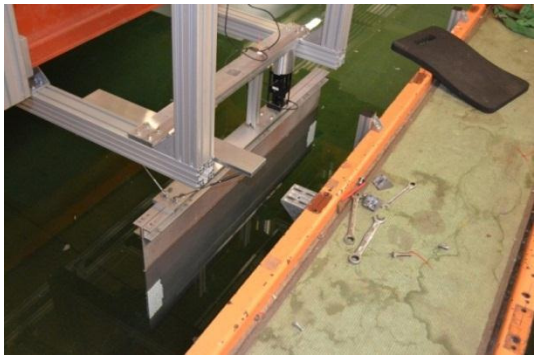

Fig. 13 – Plate 7.

4. Test Methodology

The test methodology followed in this paper is similar to that used by Schultz [7]. The Reference Plate was first towed repeatedly and the alignment of the plates adjusted until the side force was effectively zero. Once this was achieved, no further adjustments were made to the alignment over the course of the experiments. The side force of the plate was monitored for each run to ensure this alignment was maintained.

The total resistance (drag) of a flat plate, R_T, is mainly composed of two components; the residuary resistance, R_R, and the frictional resistance, R_F, as given by equation (1).

$$R_T = R_R + R_F \tag{1}$$

The residuary resistance occurs due to the wavemaking resistance and pressure resistance of the plates, while the frictional resistance arises due to shear stresses on the plate surface. It is of note that in this case, the pressure drag is expected to be negligible since the thickness of the plates is only 5mm. The surface roughness affects only skin friction resistance, which is equivalent to flat plate frictional resistance.

Once the total drag, R_T, values are obtained for each plate and related speeds, they were non-dimensionalised by dividing each term by the dynamic pressure and wetted surface area of the plates. The total drag coefficient, C_T, was therefore evaluated using the following equation (2)

$$R_T = \frac{1}{2}\rho S C_T V^2 \tag{2}$$

where ρ is the density of water, S is the wetted surface area, C_T is the total resistance coefficient and V is the speed.

5. Repeatability and Uncertainty Estimates

Uncertainty estimates for the drag coefficients and roughness function calculations were made through repeatability tests using the procedure defined by the ITTC [9]. The uncertainty estimates for any quantity can be defined as below [9]:

$$\left(U_A\right)^2 = \left(B_A\right)^2 + \left(P_A\right)^2 \tag{3}$$

where U_A is the total uncertainty, B_A is the total bias limit and P_A is the precision limit for the quantity A. B_A can also be called systematic errors and occurs due to the errors of measurement devices; it can be calculated as:

$$\left(B_A\right)^2 = \left(\frac{\partial A}{\partial x}B_x\right)^2 + \left(\frac{\partial A}{\partial y}B_y\right)^2 + \left(\frac{\partial A}{\partial z}B_z\right)^2 + \ldots \tag{4}$$

where

$$A = f(x, y, z, \ldots) \tag{5}$$

P_A is caused by random errors with regards to the repeatability of the experiment and it can be calculated by (6) for multiple tests and (7) for a single run as follows:

$$P(M) = \frac{KSDev}{\sqrt{M}} \tag{6}$$

$$P(S) = KSDev \tag{7}$$

where *K* is the coverage factor (this may be assumed to be 2 according to the ITTC [9] for 95% confidence level), *M* is the number of runs and *SDev* is the standard deviation established by multiple runs, as given below.

$$SDev = \left[\frac{\sum_{k=1}^{M}\left(A_k - A_{average}\right)^2}{M-1}\right]^{\frac{1}{2}} \tag{8}$$

The details of the procedures to carry out an uncertainty analysis can be found in ITTC [9] and Coleman and Steele [10]. The repeatability tests were performed at two speeds, namely

1.857 m/s and 3.591 m/s, which correspond to Reynolds numbers of ~$2.6x10^6$ and ~$5x10^6$, respectively.

The bias uncertainty in C_T ranged from ±1.625% at the lower Reynolds number to ±0.368% at the higher Reynolds number, while the precision uncertainty in C_T ranged from ±0.743% at the lower Reynolds number to ±0.041% at the higher Reynolds number. The overall uncertainty in C_T ranged from ±1.787% at the lower Reynolds number to ±0.430% at the higher Reynolds number.

The overall uncertainty levels of the drag coefficients are sufficient when compared to other experiments given in the literature such as Schultz [7]. The very small precision limits reveal the acceptable repeatibility of the experiments.

6. Results

Having presented the necessary uncertainty estimates, this section addresses the results of the resistance tests.

The changes in the C_T values of the test plates with respect to the Reference Plate 1 and Reference Plate 2 are given in Table 1 and Table 2, respectively, while these changes are graphically shown in Fig. 14 and Fig. 15.

Table 1 – Change in C_T values of the test plates with respect to Reference Plate 1.

	Change in C_T (%) with respect to Reference Plate 1		
Speed (m/s)	**Plate 1**	**Plate 2**	**Plate 3**
1.5	31.46	59.49	98.25
1.857	30.53	59.63	99.73
2.435	37.87	71.92	112.16
3.013	39.20	74.77	118.34
3.287	39.43	76.07	118.55
3.591	40.64	76.79	121.13

Table 2 – Change in C_T values of the test plates with respect to Reference Plate 2.

	Change in C_T (%) with respect to Reference Plate 2			
Speed (m/s)	**Plate 4**	**Plate 5**	**Plate 6**	**Plate 7**
1.5	34.93	25.36	20.60	28.51
1.857	36.07	30.06	21.71	28.27
2.435	37.86	24.43	22.23	30.15
3.013	39.46	27.61	24.09	32.70
3.287	39.16	36.24	24.25	32.47
3.591	40.60	27.19	24.39	32.52

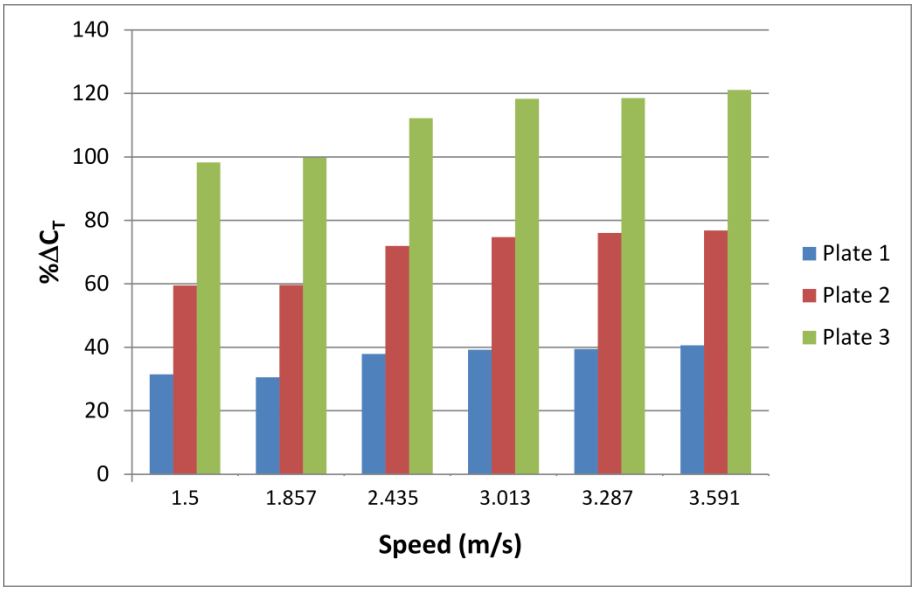

Fig. 14 – Percentage increase in C_T values of the test plates with respect to Reference Plate 1.

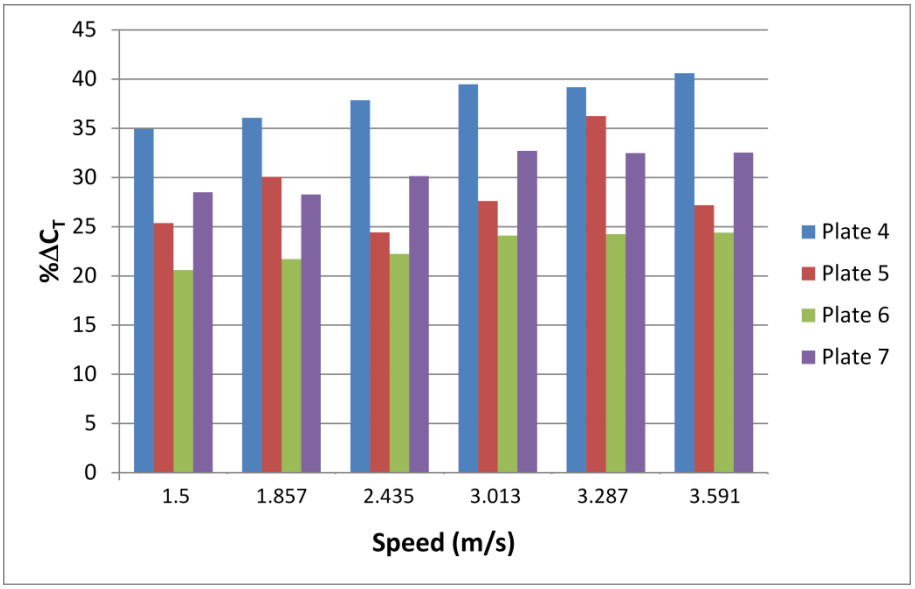

Fig. 15 – Percentage increase in CT values of the test plates with respect to Reference Plate 2.

Table 1 and Fig. 14 jointly illustrate the changes in C_T due to the varying surface coverages used in the first sets of experiments. It is clearly seen that Plate 3 corresponding to 20% coverage showed the highest drag characteristics among all of the surfaces. The increase in C_T values ranged from ~31% to ~41% for Plate 1, from ~60% to ~77% for Plate 2, from ~98% to ~121% for Plate 3 with respect to Reference Plate 1.

Table 2 and Fig. 15 show the change in C_T values due to the different fouling locations used in the second sets of experiments. It is seen that Plate 4 shows the maximum increase in drag among all the other configurations. It was very meaningful since it clearly shows the fact that the fouling accumulation on leading edge is much more important than that on other locations from drag point of view. Fouling on the leading edge can affect the flow in the first portion of the plate and it creates the turbulence in the very first portion of the flow. Hence, the shear

force stem from the turbulence manifests itself as an increased drag. The increase in C_T values ranged from ~35% to ~41% for Plate 4, ~25% to ~36% for Plate 5, from 20% to 24% for Plate 6 and from ~28% to ~32% for Plate 7.

7. Discussion and Conclusions

An experimental study of the resistance of flat plates covered with artificial barnacles was carried out. Seven flat plates having different fouling accumulation configurations were towed at the Kelvin Hydrodynamics Laboratory (KHL) of the University of Strathclyde. Also, two more bare plates were towed to obtain the base-line of the plates.

The plates were towed at a range of speeds and the total resistances of the surfaces were evaluated. The resistance values were then non-dimensionalised and presented in a comparative manner. Uncertainty estimates were made through repeatability tests and the uncertainty values were found to be sufficient enough to ensure a reliable comparison.

It is evidently seen that the coverage percentage of the barnacles significantly increase the drag of a flat plate and hence it can be claimed that it increases the frictional resistance of a ship. It is also seen that the location of the accumulation of barnacles significantly affect the increase in drag. Especially, if the fouling accumulates in the leading edge, the increase of the drag becomes more important.

A piece of future work might be to test different sizes of barnacles, to evaluate the frictional resistance coefficients from the experimental results and then to obtain the roughness function model for the tested surfaces using the method proposed by Granville [11]. It would enable us to predict the effects of fouling on the resistance of flat plates length of real ships using similarity law procedure proposed by Granville [12] or on the resistance of real ship hulls using the CFD method proposed by Demirel, et al. [4].

8. Acknowledgements

The authors gratefully acknowledge that the research presented in this paper was partially generated as part of the EU funded FP7 project FOUL-X-SPEL (Environmentally Friendly Antifouling Technology to Optimise the Energy Efficiency of Ships, Project number 285552, FP7-SST-2011-RTD-1).

9. References

1. IMO, (2009), “Second IMO GHG Study”, http://www.imo.org/blast/blastDataHelper.asp?data_id=27795
2. Schultz, M. P., (2007), "Effects of coating roughness and biofouling on ship resistance and powering," Biofouling, 23(5), pp. 331-341.
3. Demirel, Y. K., Khorasanchi, M., Turan, O., and Incecik, A., (2014), "CFD approach to resistance prediction as a function of roughness," eds., Paris/France.
4. Demirel, Y. K., Khorasanchi, M., Turan, O., Incecik, A., and Schultz, M. P., (2014), "A CFD model for the frictional resistance prediction of antifouling coatings," Ocean Engineering, 89, pp. 21-31.
5. Micanti, (2013), Barnacles on a ship hull, 05.6., http://www.micanti.com/wp-content/uploads/2013/11/aangroei-commerciele-AF-na-3-maanden-2.jpg

6. Larsson, A. I., Mattsson-Thorngren, L., Granhag, L. M., and Berglin, M., (2010), "Fouling-release of barnacles from a boat hull with comparison to laboratory data of attachment strength," Journal of Experimental Marine Biology and Ecology, 392(1–2), pp. 107-114.
7. Schultz, M. P., (2004), "Frictional resistance of antifouling coating systems," Journal of fluids engineering, 126(6), pp. 1039-1047.
8. ASTM-D6990-05, (2011), "Standard Practice for Evaluating Biofouling Resistance and Physical Performance of Marine Coating Systems".
9. ITTC, (2002), "Uncertainty Analysis, Example for Resistance Test," ITTC Recommended Procedures and Guidelines, Procedure 7.5-02-02-02, Revision 01.
10. Coleman, H. W., and Steele, W. G., (1999), *Experimentation and Uncertainty Analysis for Engineers*, Wiley.
11. Granville, P. S., (1987), "Three indirect methods for the drag characterization of arbitrarily rough surfaces on flat plates," Journal of Ship Research, 31(1), pp. 70-77.
12. Granville, P. S., (1958), "The frictional resistance and turbulent boundary layer of rough surfaces," Journal of ship research, 2, pp. 52-74.